Biomedical Optics EXPRESS

Highly sensitive color-indicating and quantitative biosensor based on cholesteric liquid crystal

Yu-Cheng Hsiao,[1] Yu-Chien Sung,[1] Mon-Juan Lee,[2,3] and Wei Lee[1,*]

[1]*Institute of Imaging and Biomedical Photonics, College of Photonics, National Chiao Tung University, Guiren Dist., Tainan 71150, Taiwan*

[2]*Department of Bioscience Technology, Chang Jung Christian University, Guiren Dist., Tainan 71101, Taiwan*

[3]*mjlee@mail.cjcu.edu.tw*

**wlee@nctu.edu.tw*

Abstract: Liquid crystal (LC)-based biosensors employ highly sensitive interfaces between the alignment layers and LCs to detect biomolecules and their interactions. Present techniques based on optical texture observation of the homeotropic-to-planar response of nematic LCs are limited by their quantitative reproducibility of results, indicating that both the accuracy and reliability of LC-based detection require further improvements. Here we show that cholesteric LC (CLC) can be used as a novel sensing element in the design of an alternative LC-based biosensing device. The chirality of the vertically anchored (VA) CLC was exploited in the detection of bovine serum albumin (BSA), a protein standard commonly used in protein quantitation. The color appearance and the corresponding transmission spectrum of the cholesteric phase changed with the concentration of BSA, by which a detection limit of 1 fg/ml was observed. The optical response of the VA CLC interface offers a simple and inexpensive platform for highly sensitive and naked-eye color-indicating detection of biomolecules, and, thus, may facilitate the development of point-of-care devices for the detection of disease-related biomarkers.

OCIS codes: (160.3710) Liquid crystals; (160.1585) Chiral media; (170.0170) Medical optics and biotechnology; (230.3720) Liquid-crystal devices.

References and links

1. S. R. Kim and N. L. Abbott, "Rubbed films of functionalized bovine serum albumin as substrates for the imaging of protein–receptor interactions using liquid crystals," Adv. Mater. **13**(19), 1445–1449 (2001).
2. C.-Y. Xue and K.-L. Yang, "Dark-to-bright optical responses of liquid crystals supported on solid surfaces decorated with proteins," Langmuir **24**(2), 563–567 (2008).
3. B. H. Clare and N. L. Abbott, "Orientations of nematic liquid crystals on surfaces presenting controlled densities of peptides: amplification of protein-peptide binding events," Langmuir **21**(14), 6451–6461 (2005).
4. C.-H. Chen and K.-L. Yang, "Detection and quantification of DNA adsorbed on solid surfaces by using liquid crystals," Langmuir **26**(3), 1427–1430 (2010).
5. V. K. Gupta, J. J. Skaife, T. B. Dubrovsky, and N. L. Abbott, "Optical amplification of ligand-receptor binding using liquid crystals," Science **279**(5359), 2077–2080 (1998).
6. T. S. Wong, T. H. Chen, X. Shen, and C. M. Ho, "Nanochromatography driven by the coffee ring effect," Anal. Chem. **83**(6), 1871–1873 (2011).
7. H.-W. Su, Y.-H. Lee, M.-J. Lee, Y.-C. Hsu, and W. Lee, "Label-free immunodetection of the cancer biomarker CA125 using high-Δ*n* liquid crystals," J. Biomed. Opt. **19**(7), 077006 (2014).
8. S.-H. Sun, M.-J. Lee, Y.-H. Lee, W. Lee, X. Song, and C.-Y. Chen, "Immunoassays for the cancer biomarker CA125 based on a large-birefringence nematic liquid-crystal mixture," Biomed. Opt. Express **6**(1), 245–256 (2015).
9. H.-W. Su, M.-J. Lee, and W. Lee, "Surface modification of alignment layer by ultraviolet irradiation to dramatically improve the detection limit of liquid-crystal-based immunoassay for the cancer biomarker CA125," J. Biomed. Opt. **20**(5), 057004 (2015).
10. P. G. De Genes and J. Prost, *The Physics of Liquid Crystals* (Oxford University Press, 1993), 2nd ed., Chap. 6.
11. Y.-C. Hsiao, C. Y. Tang, and W. Lee, "Fast-switching bistable cholesteric intensity modulator," Opt. Express **19**(10), 9744–9749 (2011).

#250493 Received 21 Sep 2015; revised 10 Nov 2015; accepted 18 Nov 2015; published 23 Nov 2015

12. Y.-C. Hsiao and W. Lee, "Lower operation voltage in dual-frequency cholesteric liquid crystals based on the thermodielectric effect," Opt. Express **21**(20), 23927–23933 (2013).
13. Y.-C. Hsiao and W. Lee, "Electrically induced red, green, and blue scattering in chiral-nematic thin films," Opt. Lett. **40**(7), 1201–1203 (2015).
14. Y.-C. Hsiao and W. Lee, "Polymer stabilization of electrohydrodynamic instability in non-iridescent cholesteric thin films," Opt. Express **23**(17), 22636–22642 (2015).
15. Y.-C. Hsiao, C.-Y. Wu, C.-H. Chen, V. Ya. Zyryanov, and W. Lee, "Electro-optical device based on photonic structure with a dual-frequency cholesteric liquid crystal," Opt. Lett. **36**(14), 2632–2634 (2011).
16. Y.-C. Hsiao, C.-T. Hou, V. Ya. Zyryanov, and W. Lee, "Multichannel photonic devices based on tristable polymer-stabilized cholesteric textures," Opt. Express **19**(24), 23952–23957 (2011).
17. Y.-C. Hsiao, Y.-H. Zou, I. V. Timofeev, V. Ya. Zyryanov, and W. Lee, "Spectral modulation of a bistable liquid-crystal photonic structure by the polarization effect," Opt. Mater. Express **3**(6), 821–828 (2013).
18. D. A. Winterbottom, R. Narayanaswamy, and I. M. Raimundo, Jr., "Cholesteric liquid crystals for detection of organic vapours," Sens. Actuators B Chem. **90**(1-3), 52–57 (2003).
19. T. R. Woliński and W. J. Bock, "Cholesteric liquid crystal sensing of high hydrostatic pressure utilizing optical fibers," Mol. Cryst. Liq. Cryst. **199**(1), 7–17 (1991).
20. H. K. Bisoyi and Q. Li, "Light-directing chiral liquid crystal nanostructures: From 1D to 3D," Acc. Chem. Res. **47**(10), 3184–3195 (2014).
21. L. Wang, H. Dong, Y. Li, R. Liu, Y. F. Wang, H. K. Bisoyi, L. D. Sun, C. H. Yan, and Q. Li, "Luminescence-driven reversible handedness inversion of self-organized helical superstructures enabled by a novel near-infrared light nanotransducer," Adv. Mater. **27**(12), 2065–2069 (2015).
22. Y.-J. Liu, P.-C. Wu, and W. Lee, "Spectral variations in selective reflection in cholesteric liquid crystals containing opposite-handed chiral dopants," Mol. Cryst. Liq. Cryst. (Phila. Pa.) **596**(1), 37–44 (2014).
23. D. Patko, K. Cottier, A. Hamori, and R. Horvath, "Single beam grating coupled interferometry: high resolution miniaturized label-free sensor for plate based parallel screening," Opt. Express **20**(21), 23162–23173 (2012).

1. Introduction

Since Abbott's group demonstrated the use of a single-compound nematic liquid crystal (LC) known as 5CB in the detection of biomolecules [1], LC-based biosensors have received much attention [2–4]. Biomolecules immobilized or adsorbed on substrate surfaces trigger the homeotropic-to-planar reorientation of nematic LC molecules [4], which can be observed through the dark-to-bright optical response of LCs under an optical microscope equipped with crossed polarizers [5]. The reorientation of LC molecules can be described by the molecular theory of surface tension, in which the critical surface tension γ_c is introduced as the criterion for homeotropic or homogeneous alignment [6]. Currently, LC-based biosensing is applied in the detection of enzymatic reactions, antibody–antigen immunoreactions, DNA hybridization, and the like [1,3,4]. Our previous studies established that the sensitivity of LC-based immunodetection for the cancer biomarker CA125 can be significantly enhanced by using a eutectic nematic LC with a wide nematic range (<–30–95 °C compared with 5CB having a narrow nematic range of ~24–35 °C) and large birefringence (Δn = 0.333 at 589 nm and 20 °C) [7–9]. Nevertheless, present techniques based on optical texture observation are limited by the non-uniformity of LC textures, which are difficult to reproduce and hard to be quantitated.

Cholesteric liquid crystals (CLCs) are a specific category of LC materials that exhibit unique physical properties such as optical bistability, Bragg reflection, and flexibility [10]. The helical structure of CLCs selectively reflects the component of light with the same handedness as the CLC chirality. Furthermore, both the helical planar (P) state and scattering focal conic (FC) state are optically bistable, suggesting that no power is required to retain the optical states of CLCs [11]. The intrinsic optical activity of CLCs facilitates the development of optoelectronic [12–14] and photonic devices [15–17], as well as detectors of low power consumption for organic vapors [18] or high hydrostatic pressure [19]. Recently stimuli-responsive CLCs and their possible applications have been explored [20,21]. Despite their extensive application, the potential of CLCs in biosensing has not been fully investigated. In this work, a simple and unique CLC-based biosensor was developed by exploiting the highly sensitive interface between CLC molecules and vertical alignment layers consisting of *N*,*N*-dimethyl-*n*-octadecyl-3-aminopropyltrimethoxysilyl chloride (DMOAP) to detect various concentrations of bovine serum albumin (BSA), a common protein standard. A schematic of this vertically anchored cholesteric (VAC) biosensor is shown in Fig. 1. In the absence of biomolecules, CLC molecules are aligned vertically near the substrates by DMOAP and the

#250493 Received 21 Sep 2015; revised 10 Nov 2015; accepted 18 Nov 2015; published 23 Nov 2015

bulk is in the hybrid FC/P state through self-assembly in the space away from the substrates, resulting in the configuration of major reflection. When the biomolecules are adsorbed on the DMOAP-coated surface, the vertical anchoring strength of the CLCs is weakened, allowing CLC molecules to transfer to the P structure and, in turn, giving rise to the major-transmission mode. The transition of the CLC structure from major reflection to major transmission caused by increasing amount of biomolecules renders the color-indicating properties of CLCs. Quantitation of the BSA concentration with a lower limit of ~1 fg/ml can be achieved by measuring the surface-induced ordering transition of CLCs through transmission spectroscopy. This study unambiguously demonstrates that CLCs are advantageous in the development of highly sensitive, color-indicating and quantitative biosensing technique.

2. Experiment

The CLC material used in this study is a blend of a nematic LC (E44, Merck) as the host and a chiral dopant (R5011, Merck) at a concentration of 2.6 wt%. The helical pitch of the resulting CLC is *ca.* 370 nm. The vertical alignment agent dimethyloctadecyl[3-(trimethoxysilyl)propyl] ammonium chloride (DMOAP) and BSA were purchased from Sigma–Aldrich. Prior to the assembly of LC cells, cleaned glass slides were immersed in an aqueous solution containing 1% DMOAP for 15 min at room temperature, rinsed with DI water for 1 min to remove excess DMOAP solution, dried under a stream of nitrogen, and finally heated at 100 °C for 15 min. BSA immobilization was performed by immersing DMOAP-coated glass slides in aqueous solution of BSA at the desired concentration for 2 h, followed by drying overnight at room temperature. To fabricate a VAC cell, ball spacers of ~5 μm in diameter mixed with ethanol were dispensed on the four corners of one of the DMOAP- and BSA-coated glass slides, which was then covered with another glass slide with the same coating, and then partially sealed with glue to form a glass-air-glass cell. Finally, the empty cell was filled with CLC by capillary action to form a VAC cell. A polarized optical microscope (POM; Olympus, Tokyo, Japan, BX51) used in this study for texture observation is equipped with a halogen lightbulb as the light source (Philips projection lamp type 7023, 12 V, 100 W). The transmission spectra of the VAC cells were acquired with a high-resolution fiber-optic spectrometer (Ocean Optics HR2000+).

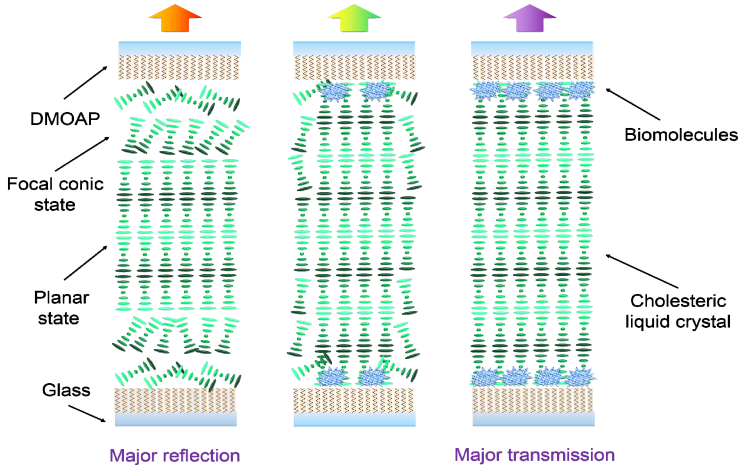

Fig. 1. Schematic of the CLC structures in a VAC biosensor. The configuration shifts from the major-reflection to the major-transmission mode in the presence of significantly abundant biomolecules.

#250493 Received 21 Sep 2015; revised 10 Nov 2015; accepted 18 Nov 2015; published 23 Nov 2015

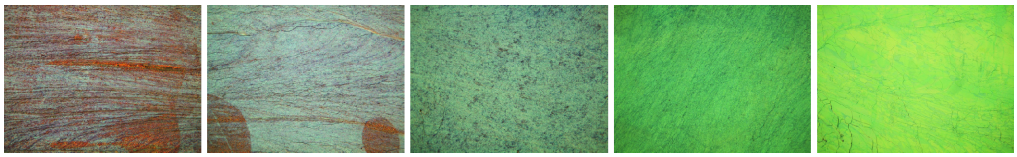

Fig. 2. POM images of VAC cells prepared with various concentrations (0 to 1 mg/ml) of BSA immobilized atop the DMOAP layers.

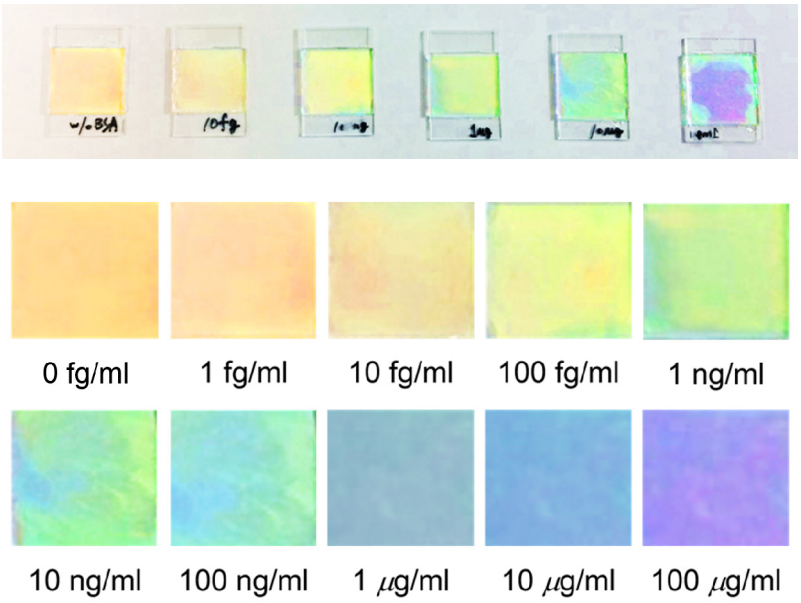

Fig. 3. Representative VAC cells featuring the color-indicating properties of the VAC biosensor at different BSA concentrations.

3. Results and discussion

The optical textures of five VCA cells in the absence and presence of various concentrations of BSA are shown in Fig. 2. The brightness of the optical texture increased with increasing concentration of BSA, accompanied by a change in color depending on the orientation of the CLC. In addition, the amount of defect lines in the optical texture, as a result of light scattering caused by the quasi-random CLC structure, was reduced when the BSA concentration was increased. Since the chiral dopant used in this study is almost temperature-independent [22], experimental results from the VAC biosensor can be conveniently and consistently reproduced in a reasonably wide range of ambient temperature. The fact that the chiral pitch of the concocted CLC is not thermosensitive is certainly advantageous for the biosensing purpose.

Representative VAC cells with 0 to 1 mg/ml immobilized BSA are shown in Fig. 3 (top row). At each BSA concentration, a distinct color was reflected from the VAC cell. The difference in color can be clearly distinguished at the center area of each VAC cell (Fig. 3). In the absence of BSA, the reflected color was orange, which then shifted from yellow to green, blue and purple with increasing concentrations of BSA. It is thus possible to determine the amount of biomolecules in the order of magnitudes or logarithmic scale by exploiting the color-indicating properties of VAC cells. The reflected color of the VAC cell at different BSA concentrations depends on the extent to which the structure of CLC is converted from the FC/P state to the P state by interacting with BSA. In the absence of BSA, the VAC cell was in the major-reflection mode (Fig. 4). Light entering the upper substrate of the VAC cell was

#250493 Received 21 Sep 2015; revised 10 Nov 2015; accepted 18 Nov 2015; published 23 Nov 2015

reflected by the partial FC structure of CLC, while transmitted purple/blue light (complementary color of orange/red) through the portion of the P structure was scattered by the FC layer on the lower substrate, resulting in the orange/red appearance of the VAC cell. In the presence of BSA, the vertical anchoring force due to DMOAP was diminished by the immobilized BSA. More CLC molecules were assembled to the P state with increasing concentration of BSA, eventually leading to the perfect planar state and the mode of major transmission, in which a half of circularly polarized orange/red light was reflected on the basis of the pitch of the CLC. Noticeably, the appearance of the VAC cell became the complementary color (i.e., purple) in that the white paper underneath the cell transmitted the purple/blue light (Fig. 4).

To develop a quantitative method for the VAC biosensor, the transmission spectra of VAC optical cells coated with various concentrations of BSA were analyzed. As shown in Fig. 5, the overall transmittance of the VAC cell ascended and reflection bandwidth decreased with increasing BSA concentration, suggesting that the distribution of the helical pitch and the effective pitch length of the CLC varied sensitively with the amount of immobilized BSA. The limit of detection of the VAC biosensor was determined to be 1 fg/ml BSA. At low BSA concentrations, the CLC in the vicinities of both the upper and lower glass substrates were in the FC state, which resulted in light scattering that rendered the Bragg reflection insignificantly. As the amount of BSA increased, the P state of CLC molecules predominated, and the optical response of the VAC cell was governed by the Bragg reflection. Consequently, the photonic band gap increased with increasing BSA concentration. When the minimum transmittance and bandwidth at half maximum of the Bragg reflection are plotted against BSA concentration in the logarithmic scale, a positive and negative correlation can be observed, respectively (Fig. 6). These results suggest that the Bragg reflection of CLCs as revealed in the transmission spectrum can be exploited in the detection and quantitation of biomolecules. Besides, calibration curves for protein quantitation can be readily generated using parameters of the Bragg reflection.

Compared with grating coupled interferometry (GCI), the most sensitive label-free device available commercially that utilizes phase-modulated evanescent waves with a voltage-driven LC modulator [23], the current VAC biosensing technique requires further improvements to become a rapid, in situ technique with linear response. Nevertheless, the potential of the electro-optical properties of LCs in biosensing has not been fully explored. With the sensitive response of LCs to the concentration and binding of biomolecules, we believe that, by proper design of the detection platform and adjustment in the quantitative parameters, several drawbacks of the current LC-based biosensing technology can be overcome in the near future.

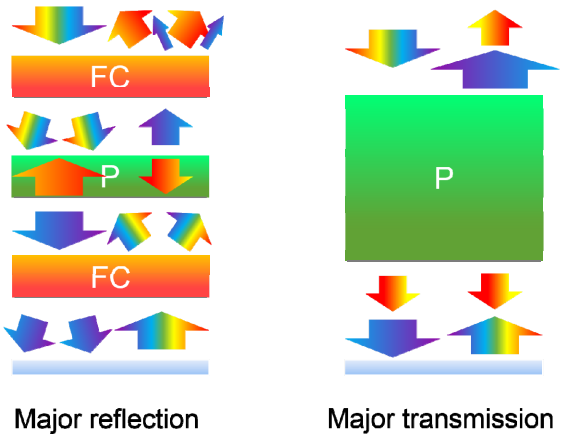

Fig. 4. The optical mechanism of the VAC biosensor in both major reflection and transmittance modes.

#250493 Received 21 Sep 2015; revised 10 Nov 2015; accepted 18 Nov 2015; published 23 Nov 2015

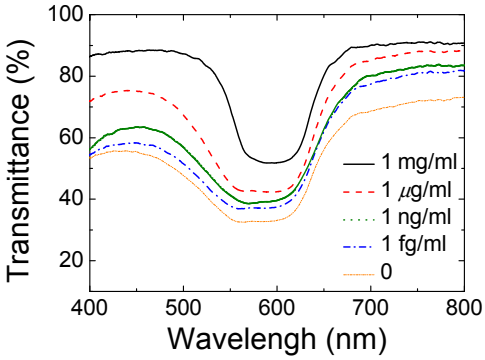

Fig. 5. The transmission spectra of VAC cells prepared with various concentrations of BSA.

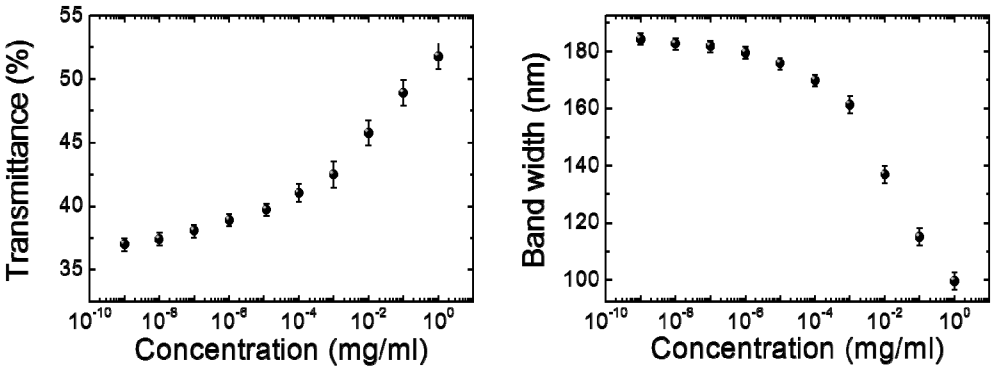

Fig. 6. Correlations of minimum transmittance and bandwidth of Bragg's reflection to BSA concentration.

4. Conclusions

We have proposed a novel and reliable VAC biosensing technique for the detection and quantitation of proteins by employing a chiral anisotropic agent; i.e., CLC. The chirality of the vertically aligned CLC molecules was sensitive to the amount of immobilized BSA on the alignment layer, which in turn affected the reflection and transmission of light, leading to the color-indicating feature of the VAC biosensor. We also demonstrated a quantitative method, which is accurate at least to the logarithmic scale, by correlating BSA concentration with the spectral properties of CLC through spectrophotometric measurements. All of the data can be easily reproduced. The detection limit of the VAC biosensor is 1 fg/ml BSA, obviously outperforming conventional methods based on texture observations and unmodified alignment layers. Further improvement can be made by decreasing the concentration of the chiral dopant, allowing the Bragg reflection to take place in the red for a resultant full spectrum of color appearances in the label-free detection (see Fig. 3). In addition, optimal thickness can be sought for the best contrast in the comparison (see Fig. 5). The VAC biosensor developed in this study offers a simple and inexpensive platform for highly sensitive and naked-eye color-indicating detection of biomolecules. It thus may facilitate the development of point-of-care devices for the detection of disease-related biomarkers.

Acknowledgments

This work was financially supported by the Ministry of Science and Technology, Taiwan, under grant Nos. 104-2112-M-009-008-MY3 and 103-2633-B-309-001. W. Lee is the corresponding author and M.-J. Lee is the co-corresponding author.

#250493 Received 21 Sep 2015; revised 10 Nov 2015; accepted 18 Nov 2015; published 23 Nov 2015